Photodissociation Studies of Mass-Selected Complex Cations Mg^+(*N*,*N*-dimethylformamide)$_{1,2}$

Haichuan Liu, Yihua Hu, and Shihe Yang*

Department of Chemistry, The Hong Kong University of Science and Technology, Clear Water Bay, Kowloon, Hong Kong, China

Received: July 18, 2003; In Final Form: September 26, 2003

Gas-phase complexes $Mg^+-[HCON(CH_3)_2]_{1,2}$ are mass-selected and studied by ultraviolet laser photodissociation in a time-of-flight mass spectrometer. Beside the dominant evaporation photofragments, some photoreaction products have also been detected from both complexes. Quantum mechanics calculations and deuterium-substitution experiments are employed to facilitate the structural, energetic, and mechanistic analysis of the photoreactions. For the most stable structures of the complexes, Mg^+ is linked to the carbonyl oxygen atoms and situated trans to the $-N(CH_3)_2$ groups. Starting from these complex structures, photoproducts are generated through (1) H abstraction next to the carbonyl group by the photoexcited Mg^{+*} (to form $(CH_3)_2NCO^+$) and/or (2) the subsequent CO loss (to form $CH_3NH^+{=}CH_2$). For $Mg^+-[HCON(CH_3)_2]_2$, the further solvation tends to hold back the photoreactions because of the even more facile evaporation channels.

Introduction

There have been considerable research activities in the photodissociation of complexes containing alkaline earth metal cations and small, common molecules.[1] The goal is to understand the molecular interactions in the complexes and evolution of these interactions under successive microsolvation.[2−4] Most recently, we have been interested in the activation of organic molecules by the electrostatically bound, photoexcited metal cations in a controlled fashion.[4,5] Photoinduced reactions have been observed in many complexes we have studied. In some cases, photoproducts are exclusive or predominant in a broad range of photolysis wavelengths.[5a,b] In other cases, pronounced product specificity on the excitation wavelength has been observed.[5c,d] Although complexes of relatively small molecules are more amenable to the detailed spectroscopic and dynamic investigations, an emerging interesting issue is to extend the photodissociation studies to large, particularly biologically important molecules. By binding a cationic metal chromophore to the large molecules at a specific site, one hopes to study the photoinduced energy transfer, electron transfer, and effective activation of molecules that lead to the rearrangement of the nuclear framework. Furthermore, the previous photodissociation studies of small ion−molecule complexes provide a good basis for comparison.

Formamide ($HCONH_2$) is the simplest prototype of a peptide linkage. High-energy barriers have been spotted for the conversion to the tautomers formamidic acid (HN═CHOH) and (aminohydroxy)carbene (H_2NCOH) (45−84 kcal/mol).[6−8] Tortajada and co-workers have studied the association complexes M^+−formamide (M = Cu, Ni, Li, Mg, Al, Ag) using the mass-analyzed ion kinetic energy (MIKE) spectrometry and collision-activated dissociation (CAD) techniques.[7−13] In what was found to be the most stable structure of M^+−formamide, the metal ion is attached to the carbonyl oxygen and trans to the $-NH_2$ group. However, the corresponding cis conformer is less stable by only a few kcal/mol (e.g., 2.3 kcal/mol for M = Cu),[9] and the cis−trans isomerization involves a very low energy barrier (1.9 kcal/mol). On the other hand, the structures of M^+-(HN═CHOH) and $M^+(H_2N-C-OH)$ were found to be much less stable than M^+−formamide.[7−12] The intra-complex reactions of M^+−formamide (M = Cu or Ni) involve the 1,2-H shift from C to O, followed by the formations of a series of intermediates in which M^+ binds to the carbene center.[9,10] In most cases, the resulting products are obtained, in which M^+ is bi-coordinated by two closed-shell molecules, such as NH_3 and CO or H_2O and HNC/HCN. Although the C−N insertion-type mechanism was found to be not possible for Cu^+−formamide, it is favorable in the case of Ni^+−formamide, which leads to CO loss.

Here we report a photodissociation study of the complexes between Mg^+ and monomer/dimer of a formamide derivative, *N*,*N*-dimethylformamide [$HCON(CH_3)_2$] (DMF). DMF is interesting in that it is actually a more authentic mimicry of peptide bonds than formamide; the $-N(CH_3)-CO-$ moiety can be viewed as a building block of a N-substituted peptide. Furthermore, photodissociation dynamics of free DMF has attracted much attention during the last few decades.[14−18] The ruptures of the two types of C−N bonds are found to be major pathways in the photodissociation of DMF, whereas the breakage of the (O)C−H bonds is much less probable. It is motivating to see how the photodissociation occurs in the complexes, in which the metal cation may bind preferentially to the carbonyl O site. Another consideration for the choice of DMF is to rule out the possible tautomerizations that may convert Mg^+−formamide to Mg^+(HN═CHOH) or $Mg^+(H_2NCOH)$,[8] due to the absence of the N−H bonds. It is anticipated that the complex structures play a crucial role in the photoreaction dynamics of the microsolvated systems.

Experiments and Calculations

Details about the cluster apparatus can be found elsewhere.[4] A brief description relevant to the present experiments is given here. A motor-driven rotating magnesium rod (ϕ5 mm × 5 cm)

* To whom correspondence should be addressed. E-mail: chsyang@ust.hk.

10.1021/jp036110k CCC: $25.00
Published on Web 10/31/2003

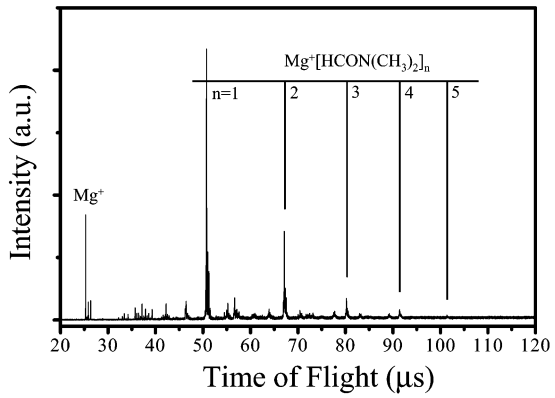

Figure 1. Mass spectrum of clusters Mg^+(*N*,*N*-dimethylformamide)$_n$ (n = 1−5). The experimental condition was optimized for larger clusters.

was mounted 15 mm downstream from the exit of a pulsed valve (General Valve). The sample rod was rotated and translated on each laser pulse to expose fresh surfaces for laser ablation. Cluster beams of DMF were generated by the pulsed valve via supersonic expansion of the vapor seeded in helium with a backing pressure of ∼40 psi through a 0.5 mm diameter orifice. The second harmonic (532 nm) of a Nd:YAG laser (∼40 mJ/pulse) was weakly focused on a ∼1 mm diameter spot of the magnesium disk for the generation of metal cations. The laser-produced species containing metal ions and atoms traversed perpendicularly to the supersonic jet stream 20 mm from the ablation sample target, forming a series of metal cations solvated by two title molecules. The nascent complexes and clusters then traveled 14 cm down to the extraction region of the reflectron time-of-flight spectrometer (RTOFMS).

The cation−molecule complexes were accelerated vertically by a high voltage pulse in a two-stage extractor. After extraction, the cluster cations were steered by a pair of horizontal plates and a pair of vertical deflection plates. All of the cluster cations were reflected by the reflectron and finally detected by a dual-plate microchannel plate detector (MCP). For photodissociation experiments, a two-plate mass gate equipped with a high-voltage pulser was used to select desired cluster cations. The mass-selected cluster cations, once arrived at the turn-around region of the reflectron, were irradiated with a collimated beam of a dye laser for photolysis. The parent and nascent daughter cations were re-accelerated by the reflectron electric field and detected by the MCP detector. The dye laser was pumped by a XeCl excimer laser (Lambda-Physik LPX210i/LPD3002). The spectral region of 335−450 nm was covered by the fundamental outputs of the dye laser using *p*-terphenyl, DMQ, BBQ, Stilbene 1, and Coumarin 440. For the spectral region of 230−270 nm, the second harmonic outputs were employed using Coumarin 503 and Coumarin 480.

Ground-state structures of the parent complexes and their photofragments ($C_2H_6N^+$ and $C_3H_6NO^+$) were computed at the B3LYP/6-31+G** level using the Gaussian 98 package.[19] Zero-point energy (ZPE) correction has been taken into account.

Results and Discussion

A. Photodissociation Patterns. Figure 1 shows a typical mass spectrum of micro-solvated magnesium cations $Mg^+[HCON(CH_3)_2]_n$ (n = 1−5). With the increase of the solvation number n, the intensity of the cationic clusters decreases gradually. The mass peaks of $Mg^+[HCON(CH_3)]_{1,2}$ can be easily selected and subject to the photolysis studies. Selected photodissociation difference mass spectra of $Mg^+[HCON(CH_3)_2]$ at short (∼350 nm) and long (∼250 nm) wavelengths are each displayed in Figure 2a,b. In general, the evaporation of Mg^+ is the predominant energy relaxation channel. However, some photoproducts are also detected such as $CH_3NH^+{=}CH_2$ and $(CH_3)_2NCO^+$ with the latter being observed only in the long wavelength region by the loss of MgH. In addition, a minor peak at m/z = 27 is assigned to $^{26}MgH^+$. To ascertain the origin of the H atom in MgH and MgH^+, the photodissociation experiment was extended to $Mg^+[DCON(CH_3)_2]$ under identical experimental conditions. As shown in Figure 2a′,b′, it is remarkable that, with a single D substitution in HCO, no photoproduct other than the evaporation photofragment Mg^+ was observed in both the long and short wavelength regions. This is a strong indication that the abstracted H atom after photo-

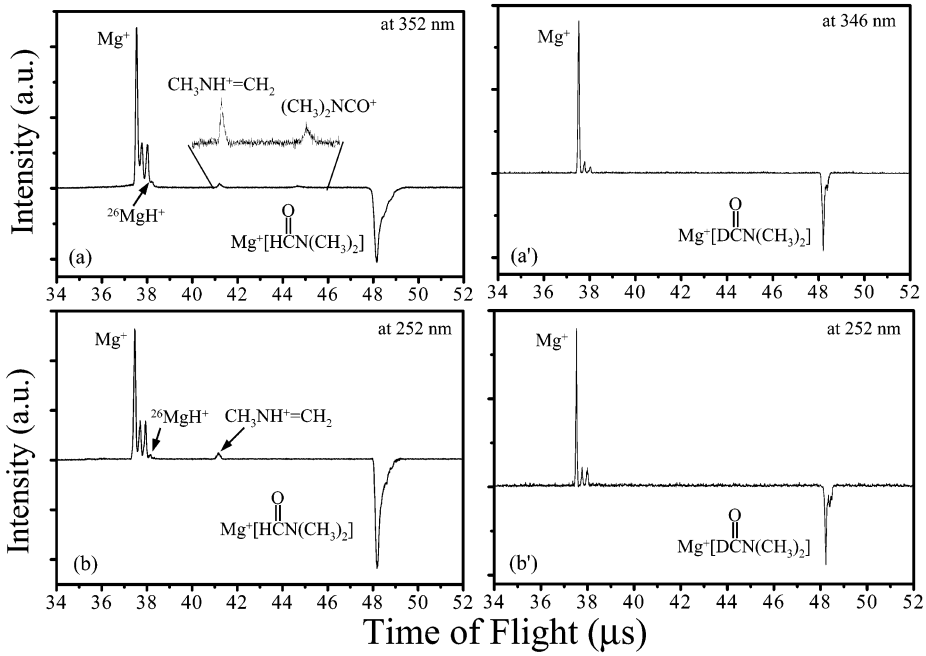

Figure 2. Photodissociation difference mass spectra of mass-selected complexes $Mg^+[HCON(CH_3)_2]$ and $Mg^+[DCON(CH_3)_2]$ in the long (a and a′) and short (b and b′) wavelength regions. The inset of a shows an expanded view of two photoproducts.

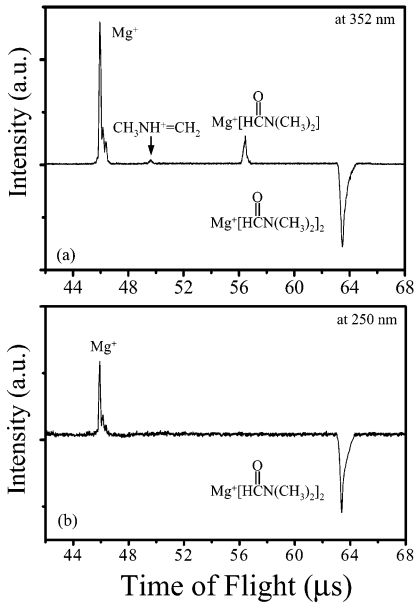

Figure 3. Photodissociation difference mass spectra of $Mg^+[HCON(CH_3)_2]_2$ at 352 nm (a) and at 250 nm (b).

dissociation of $Mg^+[HCON(CH_3)_2]$ is from HCO rather than from CH_3. More discussion on the photoreaction mechanism will follow below.

The photolysis patterns of $Mg^+[HCON(CH_3)_2]_2$ are shown in Figure 3. In the long wavelength region, the losses of a single and two units of $HCON(CH_3)_2$ both take place (Figure 3a). The photoproduct $CH_3NH^+{=}CH_2$ is also observed although it is minor. As will be described below, this peak is believed to be from a two-photon process because the energy required for the cation generation is rather high (~5.42 eV) according to our calculation. In the short wavelength region, only the evaporation photofragment Mg^+ appears (Figure 3b). It seems that the photoevaporation competes strongly with the photoinduced H-abstraction pathway.

B. Structure Calculations. The optimized structures of **1**−**4** are shown in Figure 4. The parent complexes $Mg^+[HCON(CH_3)_2]_{1,2}$ (**1** and **2**) are coordinated to Mg^+ through the carbonyl oxygen on the C−H side of the HCO groups with resulting symmetries of C_s (**1**) and C_{2v} (**2**), respectively. As expected, no local minimum is located where direct interaction between Mg^+ and the nitrogen atom is involved. Moreover, with a starting structure of $Mg^+[HCON(CH_3)_2]$ in which Mg^+ approaches O on the N−CH_3 side, the optimization lead to the structure **1**. Such a C_s structure has also been found by Armentrout and co-workers for $Na^+[HCON(CH_3)_2]$.[13] On the coordination to Mg^+, the C=O bond is lengthened to 1.269 Å (**1**) and 1.261 Å (**2**) from 1.224 Å, whereas the HC−N bond is significantly shortened to 1.316 Å (**1**) and 1.324 Å (**2**) from 1.364 Å. These bond length changes result from the charge re-distribution influenced by Mg^+. The effect of the ligand on the atomic charge of Mg^+ is approximately cumulative. For example, the atomic charge of Mg^+ is reduced from +1 (Mg^+) to +0.754 (**1**) to +0.499 (**2**) owing to the successive electron donation from O. However, the metal−ligand interaction is slightly trimmed down on successive ligand addition. This can be seen from the increased bond length of Mg^+−O in **2** (2.006 Å) compared to that in **1** (1.943 Å).

The bond dissociation energy (BDE) of **1** is calculated to be 2.39 eV, which is larger than those of Mg^+(formamide) (2.11 eV).[8] The enhanced Mg^+−O binding in **1** arises from the stronger electron donating ability of the lone pair electrons due

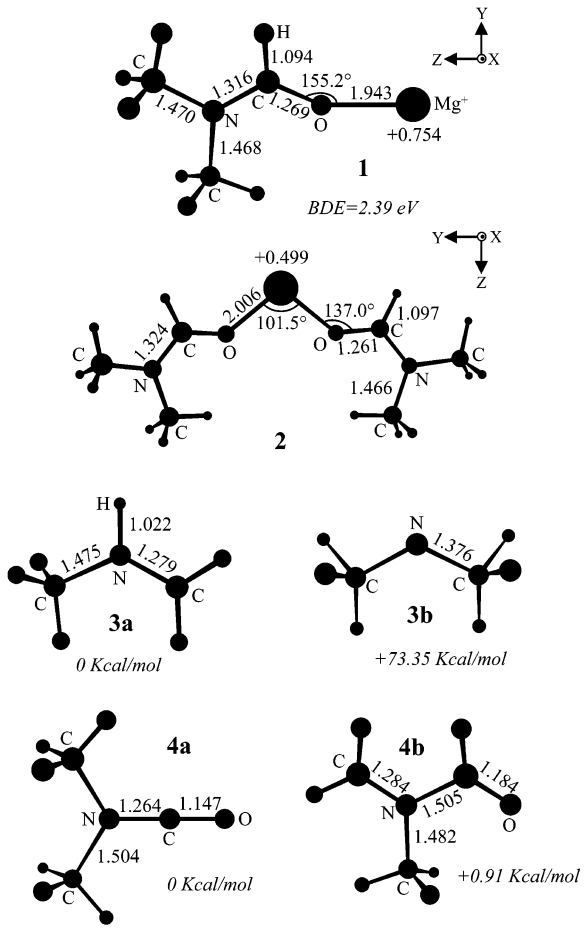

Figure 4. Optimized structures of the complexes $Mg^+[HCON(CH_3)_2]$ (**1**) and $Mg^+[HCON(CH_3)_2]_2$ (**2**), and the photoproducts (**3** and **4**). The bond lengths and bond angles are given in angstroms (Å) and degrees (°), respectively. "BDE" is abbreviation for the bond dissociation energy between Mg^+ and the molecule.

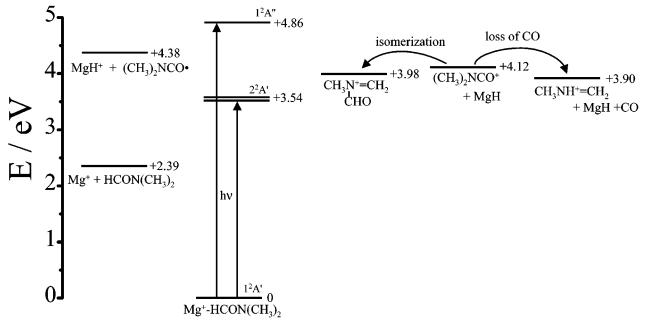

Figure 5. Energy diagram for the species involved in the photoprocesses of $Mg^+[HCON(CH_3)_2]$.

to the two methyl groups on N. For **2**, 1.52 eV is required for the ejection of the first ligand. Calculations have also been performed on the possible structures of the photoproducts observed in the present experiment, viz., **3a**, **3b** and **4a**, **4b**. For the cation at $m/z = 44$, **3a** ($CH_3{-}NH^+{=}CH_2$) is more stable than **3b** ($CH_3N^+CH_3$) by as high as 73.35 kcal/mol due to an optimized bonding geometry. However, the two candidate structures for the cation at $m/z = 72$ (**4a** and **4b**) are comparable in energy; the isocyanate cation (**4a**) is only 0.91 kcal/mol more stable than the formyl imine cation (**4b**). The energetics relevant to the photodissociation experiment is illustrated in Figure 5, which will be discussed below.

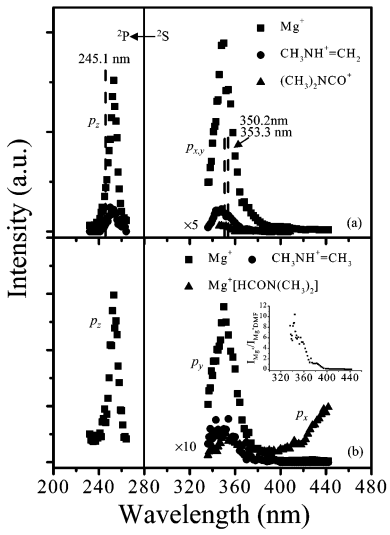

Figure 6. Action spectra for $Mg^+[HCON(CH_3)_2]$ (a) and $Mg^+[HCON(CH_3)_2]_2$ (b). The solid line indicates the atomic transition of Mg^+ ($3^2P \leftarrow 3^2S$) at 280 nm. The dashed lines denote the calculated absorption spectra employing the CIS method. Inset of b: Intensity ratio of Mg^+ to $Mg^+[HCON(CH_3)_2]$ versus wavelength for $Mg^+[HCON(CH_3)_2]_2$.

C. Photodissociation Action Spectra. Channel-resolved photodissociation action spectra of $Mg^+[HCON(CH_3)_2]$ (**1**) and $Mg^+[HCON(CH_3)_2]_2$ (**2**) are shown in Figure 6. It can be seen that the absorption spectrum of **1** (Figure 6a), calculated using CIS with the optimized ground-state structure, agrees well with the corresponding action spectra for all of the photofragments. The action spectra are characterized by two pronounced peaks around 255 and 350 nm. The absorption peaks result from the splitting of the Mg^+ 3p orbitals in the presence of ligands. The blue-shifted peak at ∼255 nm is ascribed to the transition from 3s to $3p_z$ of Mg^+ ($3^2A'$ excited-state derived from C_s symmetry), whereas the red-shifted peak at ∼350 nm is from the excitation to the $1^2A''$ and $2^2A'$ states associated with the nearly degenerate $3p_x$ and $3p_y$ orbitals, respectively. Upon the addition of one more $HCON(CH_3)_2$, the only noticeable spectral change of $Mg^+[HCON(CH_3)_2]_2$ (Figure 6b) is the appearance of an extra peak at ∼440 nm. Although spectral calculation has not been conducted on **2**, it is anticipated that, with the C_{2v} symmetry of the complex, the $3p_z$, $3p_y$, and $3p_x$ orbitals are associated with the 2^2A_1, 1^2B_2, and 1^2B_1 excited states, respectively. As such, the nearly degenerate $3p_x$ and $3p_y$ orbitals in **1** are split further in **2** due to the different coordination geometries, and the 1^2B_1 ($3p_x$) state is red-shifted significantly in the di-solvated complex by the interaction with the π^* orbital of an additional C═O. Notice that the intensity ratio of Mg^+ to $Mg^+[HCON(CH_3)_2]$ increases with the decreasing wavelength (see the inset of Figure 6b), indicating a stepwise process of evaporation. At $\lambda > 400$ nm, the dominant photofragment is the mono-solvated $Mg^+[HCON(CH_3)_2]$, whereas Mg^+ takes over at $\lambda < 370$ nm. The appearance potential of Mg^+ from $Mg^+[HCON(CH_3)_2]_2$ is estimated to be ∼3.14 eV (∼395 nm). This is substantially smaller than the corresponding value from our calculation (3.91 eV) due perhaps to the internal energies of the complexes and/or the overestimation from the calculation.

D. Mechanistic Implications of the Photoreactions. The photoinduced evaporation and reaction pathways of $Mg^+[HCON(CH_3)_2]_{1,2}$ are summarized in Figure 5 along with the calculated energetics. For the photoreactions in $Mg^+[HCON(CH_3)_2]$, the first step is the loss of H at $HCON(CH_3)_2$, forming a neutral counterpart MgH. Upon photoexcitation, Mg^+ may pick up the H at HCO by inserting the C−H bond, forming the cation $(CH_3)_2NCO^+$ at $m/z = 72$ or MgH^+ as observed. Alternatively, the insertion of Mg^+ into the C−H bond of CH_3 leads to the direct formation of $HCON^+(=CH_2)CH_3$ ($m/z = 72$), which is only ∼0.91 kcal/mol less stable than the isomer $(CH_3)_2NCO^+$. As described above, the D-substitution experiment supports the former mechanism. This is reasonable given that the H in HCO is much closer than that in CH_3. Although one could imagine a six-membered ring transition state for the abstraction of H from CH_3, it is not favorable in terms of entropy. Nevertheless, the existence of $HCON^+(=CH_2)CH_3$ for the cation at $m/z = 72$ cannot be excluded because it may come from the isomerization of the less stable $(CH_3)_2NCO^+$. The energy needed for the formation of MgH^+ is calculated to be 4.38 eV (∼283 nm), whereas the formation energy of $(CH_3)_2NCO^+$ is 4.12 eV (∼301 nm). The decomposition of $(CH_3)_2NCO^+$ to $CH_3NH^+{=}CH_2$ is exothermic by 0.22 eV. According to the above data, the photon energies are not sufficient to form these photoproducts. The fact that we have observed the photoproducts even in the long wavelength region may be due to the thermal energies of the complexes and/or the inaccuracy of the calculations. This has been pointed out above in the analysis of the evaporation channels. In the short wavelength range, $CH_3NH^+{=}CH_2$ is still observable but $(CH_3)_2NCO^+$ wades away (see Figure 2) presumably because more energy now is available for bring the CO-loss channel to completion.

For the di-solvated complex $Mg^+[HCON(CH_3)_2]_2$, the energy needed for evaporating the first solvent molecule is calculated to be 1.52 eV. Considering that the evaporation of the second solvent molecule needs 2.39 eV, the formation of Mg^+ from $Mg^+[HCON(CH_3)_2]_2$ costs ∼3.91 eV. In the long wavelength region, the cation $CH_3NH^+{=}CH_2$ was also observed (see Figures 3a and 6b). According to our calculation, the formation energy of this cation from the di-solvated complex is ∼5.42 eV (∼230 nm). It is likely that the $CH_3NH^+{=}CH_2$ is observed in the long wavelength range by two-photon absorption. However, this photoproduct is absent in the short wavelength region either because one-photon is insufficient or because the evaporation channel is much more competitive in the short wavelength region. In this sense, further solvation has the effect of reducing the probability of the photoreactions because the available energy is mainly disposed by the solvent evaporation.

The low photoproduct yields indicate that the photoreactions are not kinetically or/and energetically favored compared to the dominant evaporation channel. This can also be appreciated from the marked primary kinetic isotope effect of the photoreactions. As mentioned above, when the H atom in HCO is substituted by D, the photoreaction channels from $Mg^+[HCON(CH_3)_2]$ are beyond detection. This can be attributed to a higher energy barrier for the abstraction of D. In terms of the ZPE differences of the C−H and C−D bonds, the increase of the D-abstraction barrier may be approximated as $(1/2)h\nu_{C-H}[1 - (\mu_{CH}/\mu_{CD})^{1/2}]$. In addition, tunneling may become significant in the present case. Because the probability of tunneling through a barrier decreases as the mass of the particles increases, deuterium tunnels less efficiently than hydrogen and its reactions are slower, actually beyond detection as observed. It appears then both the increase in activation energy and decrease in tunnel probability play a role in slowing down the D abstraction. On the other hand, the evaporation might be relatively fast such that the abstraction of H can barely compete but the frustrated D abstraction is too slow to be detected under our experimental conditions. As another kinetic consideration, the chance of Mg^{+*} insertion into the C−H bond after photoexcitation of the

complexes is not high because the distance between Mg^+ and H of HCO in ground-state $Mg^+[HCON(CH_3)_2]$ is relatively large (~3.58 Å) due to the separation by the C═O double bond and a kinetic barrier is expected. Energetically, the Mg^+ insertion pathway (4.12 eV) is much more costly than the evaporation process (~2.39 eV).

The photoreaction mechanism mentioned above was invoked for the formation of MgH^+ from photodissociation of Mg^+-(aldehyde).[20,21] Here the photoproduct is also weak and dominated by the nonreactive evaporation. However, at least two differences are noticed. First, the neutral photoproduct MgH was observed from Mg^+(DMF) but not from Mg^+(aldehyde) due to the favorable immonium structure in the former case. Second, the complex binding is stronger in Mg^+(DMF) (2.39 eV) than in Mg^+(aldehyde) (1.35 eV) due to the stronger donating ability of the amino group and this may also play a role in the photoreactions.

It is interesting to compare our results with the MIKE and CID works on M^+−formamide (M = Cu or Ni).[9,10] Some distinct differences are noticed. First, the MIKE and CID of M^+−formamide (M = Cu or Ni) gave rise to the loss of HCO, H_2O, NH_3, CO, and HNC/HCN, whereas none of these can be observed in the photodissociation of Mg^+(DMF). In the cases of M^+−formamide (M = Cu or Ni), most of the reactions (loss of NH_3, CO, H_2O, and HNC/HCN) start with overcoming a high energy barrier by H shift from C to O, forming an intermediate $M^+(HO-C-NH_2)$, in which M^+ is still linked to O. The intermediate quickly isomerizes through a very low energy barrier to another intermediate $M^+[C(OH)NH_2]$, in which M^+ is now linked to the carbene center. For Mg^+(DMF), however, these intermediates are not formed. Instead, Mg^+ picks up the H in HCO. Second, the C−N bond insertion mechanism was used to explain the CO-loss process in Ni^+−formamide, but this is not observed in the photodissociation of Mg^+(DMF). Finally, the formation of Cu^+NH_2 (loss of $HCO^•$) was identified from CID of Cu^+−formamide. The product was thought of being from the existence of a less stable isomer of Cu^+−formamide, in which Cu^+ is attached to the N atom of NH_2. For Mg^+(DMF), such kinds of isomers should be very unstable due to space hindrance induced by two CH_3 groups. This agrees with the fact that $Mg^+N(CH_3)_2$ was not found in our experiment. Taken together, although the metal cations and the modes of excitation are also different for the reactions of the complexes, it seems that the two CH_3 substitutions at NH_2 of formamide have a significant influence on the reactions of M^+(formamide). The combination of our result with those from Tortajada's group should shed a light on the understanding of interaction between metal cation and peptide chain with the −NH−CO− units.

Another useful comparison is with the photodissociation of Mg^+−isocyanate.[5a] Isocyanate (C_2H_5NCO) and DMF ($HCON(CH_3)_2$) both have a NCO moiety except that the latter has an H atom connected to the carbonyl carbon. In both complexes, Mg^+ is linked to the O atom. However, the photodissociation patterns are quite different. Photoreactions in Mg^+−isocyanate involves mainly the cleavage of the $OCN-C_2H_5$ bond, whereas the carbonyl H atom is the primary target for activation in the photoreactions of $Mg^+[HCON(CH_3)_2]$.

Conclusions

The metal cation−molecule complexes $Mg^+[HCON(CH_3)_2]_{1,2}$ have been produced in a supersonic beam. By mass-selecting each complex, we have measured the relative photodissociation product yields as a function of the excitation wavelength in the ultraviolet region. It is shown that the photodissociation of $Mg^+[HCON(CH_3)_2]_{1,2}$ starts from the photoexcitation of Mg^+ ($3^2P \leftarrow 3^2S$), which triggers the subsequent evaporation and reactions. Three photoproducts, MgH^+, $CH_3NH^+{=}CH_2$, and $(CH_3)_2NCO^+$ [and/or $HCON^+(=CH_2)CH_3$] have been identified with low yields compared to the dominant evaporation photofragments Mg^+ and $Mg^+[HCON(CH_3)_2]$. Quantum mechanics calculations have been performed to obtain the ground-state structures and energetics of the complexes and the observed photoproducts. A D-substitution experiment was used to study the photoreaction mechanism. In the ground-state structures of the complexes $Mg^+[HCON(CH_3)_2]_{1,2}$, Mg^+ is linked to the carbonyl oxygen, pointing away from the CH_3 groups. We have demonstrated a new photoreaction pathway in a metalated peptide-like unit. The key step for the photoreactions is found to be the abstraction of the carbonyl H atom by the photoexcited Mg^{+*}. This is followed by the formation of MgH and MgH^+ and the loss of CO, accounting for all of the photoproducts we have observed. The photoreactions are slowed by the further solvation because of the competition of the more facile solvent evaporation channels.

Acknowledgment. This work was supported by an RGC grant administered by the UGC of Hong Kong.

References and Notes

(1) (a) Kleiber, P. D.; Chen, *J. Int. Rev. Phys. Chem*. **1998**, *17*, 1. (b) Duncan, M. A. *Annu. Rev. Phys. Chem*. **1997**, *48*, 69.

(2) (a) Sperry, D. C.; Midey, A. J.; Lee, J. I.; Qian, J.; Farrar, J. M. *J. Chem. Phys*. **1999**, *111*, 8469. (b) Lee, J. I.; Sperry, D. C.; Farrar, J. M. *J. Chem. Phys*. **2001**, *114*, 6180. (c) Lee, J. I.; Farrar, J. M. *J. Phys. Chem. A* **2002**, *106*, 11882.

(3) (a) Misaizu, F.; Sanekata, M.; Fuke, K.; Iwata, S. *J. Chem. Phys*. **1994**, *100*, 1161. (b) Sanekata, M.; Misaizu, F.; Fuke, K. *J. Chem. Phys*. **1996**, *104*, 9768. (c) Yoshida, S.; Daigoku, K.; Okai, N.; Takahata, A.; Sabu, A.; Hashimoto, K.; Fuke, K. *J. Chem. Phys*. **2002**, *117*, 8657. (d) Furuya, A.; Ohshimo, K.; Tsunoyama, H.; Misaizu, F.; Ohno, K.; Watanabe, H. *J. Chem. Phys*. **2003**, *118*, 5456.

(4) (a) Yang, X.; Liu, H. C.; Yang, S. H. *J. Chem. Phys*. **2000**, *113*, 3111. (b) Liu, H. C.; Guo, W. Y.; Yang, S. H. *J. Chem. Phys*. **2001**, *115*, 4612.

(5) (a) Sun, J. L.; Liu, H. C.; Han, K. L.; Yang, S. H. *J. Chem. Phys*. **2003**, *118*, 10455. (b) Liu, H. C.; Wang, C. S.; Guo, W. Y.; Wu, Y. D.; Yang, S. H. *J. Am. Chem. Soc*. **2002**, *124*, 3794. (c) Guo, W. Y.; Liu, H. C.; Yang, S. H. *J. Chem. Phys*. **2002**, *117*, 6061. (d) Guo, W. Y.; Liu, H. C.; Yang, S. H. *J. Chem. Phys*. **2002**, *116*, 2896.

(6) (a) Kim, Y.; Lim, S.; Kim, H. J.; Kim, Y. *J. Phys. Chem. A* **1999**, *103*, 617. (b) McGibbon, G. A.; Burgers, P. C.; Terlouw, J. K. *Int. J. Mass Spectrom. Ion Processes* **1994**, *136*, 191.

(7) Luna, A.; Morizur, J. P.; Tortajada, J.; Alcami, M.; Mo, O.; Yanez, M. *J. Phys. Chem. A* **1998**, *102*, 4652.

(8) Tortajada, J.; Leon, E.; Morizur, J. P.; Luna, A.; Mo, O.; Yanez, M. *J. Phys. Chem*. **1995**, *99*, 13890.

(9) Luna, A.; Amekraz, B.; Tortajada, J.; Morizur, J. P.; Alcami, M.; Mo, O.; Yanez, M. *J. Am. Chem. Soc*. **1998**, *120*, 5411.

(10) Rodriguez-Santiago, L.; Tortajada, J. *Int. J. Mass Spectrom*. **2002**, *12417*, 1.

(11) Boutreau, L.; Leon, E.; Luna, A.; Toulhoat, P.; Tortajada, J. *Chem. Phys. Lett*. **2001**, *338*, 74.

(12) Hoyau, S.; Ohanessian, G. *Chem. Phys. Lett*. **1997**, *280*, 266.

(13) Armentrout, P. D.; Rodgers, M. T. *J. Phys. Chem. A* **2001**, *104*, 2238.

(14) Volman, H. *J. Am. Chem. Soc*. **1941**, *63*, 2000.

(15) Livingston, R.; Zeldes, H. *J. Chem. Phys*. **1967**, *47*, 4137.

(16) Bosco, S. R.; Cisillo, A.; Timmons, R. B. *J. Am. Chem. Soc*. **1969**, *91*, 3140.

(17) Ann, Q.; Adams, J. *Int. J. Mass Spectrom*. **1991**, *107*, R1.

(18) Liu, D.; Fang, W. H.; Lin, Z. Y.; Fu, X. Y. *J. Chem. Phys*. **2002**, *117*, 9241.

(19) Frisch, M. J.; Trucks, G. W.; Schlegel, H. B.; Scuseria, G. E.; Robb, M. A.; Cheeseman, J. R.; Zakrzewski, V. G.; Montgomery, J. A., Jr.; Stratmann, R. E.; Burant, J. C.; Dapprich, S.; Millam, J. M.; Daniels, A. D.; Kudin, K. N.; Strain, M. C.; Farkas, O.; Tomasi, J.; Barone, V.; Cossi, M.; Cammi, R.; Mennucci, B.; Pomelli, C.; Adamo, C.; Clifford, S.; Ochterski, J.; Petersson, G. A.; Ayala, P. Y.; Cui, Q.; Morokuma, K.; Malick,

D. K.; Rabuck, A. D.; Raghavachari, K.; Foresman, J. B.; Cioslowski, J.; Ortiz, J. V.; Stefanov, B. B.; Liu, G.; Liashenko, A.; Piskorz, P.; Komaromi, I.; Gomperts, R.; Martin, R. L.; Fox, D. J.; Keith, T.; Al-Laham, M. A.; Peng, C. Y.; Nanayakkara, A.; Gonzalez, C.; Challacombe, M.; Gill, P. M. W.; Johnson, B. G.; Chen, W.; Wong, M. W.; Andres, J. L.; Head-Gordon, M.; Replogle, E. S.; Pople, J. A. *Gaussian 98*, revision A.7M; Gaussian, Inc.: Pittsburgh, PA, 1998.

(20) Lu, W. Y.; Kleiber, P. D. *J. Chem. Phys*. **2001**, *114*, 10288.

(21) Lu, W. Y.; Wong, T. H.; Sheng, Y.; Kleiber, P. D. *J. Chem. Phys*. **2002**, *117*, 6870.